Acta Cryst. (1978). A**34**, 603–607

Molecular Images of the Hydrocarbon $C_{22}H_{12}$ – Anthanthrene

BY J. R. FRYER

Chemistry Department, University of Glasgow, Glasgow G12 8QQ, Scotland

(*Received* 21 *November* 1977; *accepted* 15 *March* 1978)

The aromatic hydrocarbon anthanthrene ($C_{22}H_{12}$) has been imaged by high-resolution electron microscopy using minimal-exposure techniques. A simple photographic averaging technique has been applied to give structural information. The radiation sensitivity of this molecule is approximately 0·2 C cm^{-2} and it is suggested that smaller molecules of comparable sensitivity are capable of being imaged, the limitation being instrumental resolution rather than radiation sensitivity.

The hydrocarbon anthanthrene (naphtho[*b*,*c*,*d*]-pyrene) as shown in Fig. 1 crystallizes as yellow needles and has a melting point of 261 °C. No previous electron-microscope examination has been carried out and an X-ray structure determination by Smith & Stalley (1975) has shown the crystals to be monoclinic with $a = 12{\cdot}10$, $b = 10{\cdot}34$, $c = 10{\cdot}72$ Å, $\beta = 92{\cdot}2°$, space group $P2_{1/a}$ and $Z = 4$, but no details of atomic coordinates are given in the paper. The molecular dimensions given in Fig. 1 are calculated from normal aromatic C–C and C–H bond lengths with a perfectly planar aromatic molecule assumed.

Resolution of molecules of this size in the electron microscope is limited by three major factors: the resolving power of the instrument, the radiation stability of the molecule and the ability to prepare the specimen in a suitable manner. The first of these factors is easily achieved by a modern instrument which has a point-resolving power of 2·5–3 Å, but the most important criterion is the phase-contrast-transfer envelope that shows the range of spatial frequencies over which constant contrast can be achieved. This problem has been extensively studied and most aspects summarized by Cowley (1975) and Rose (1977). The shape of the molecule requires much higher resolution and within the limitations of the contrast-transfer envelope it is reasonable that normal geometric optics would apply, assuming a phase object. This problem of shape resolution was initially considered by Von Borries & Kausche (1940) for colloidal gold particles, and they derived the expression:

$$d = 2\delta \left(1 + \cos\frac{\pi}{n}\right)\left(\frac{n}{\pi}\cot\frac{\pi}{n}\right)^{\frac{1}{2}},$$

where δ is the point–point resolution, n the number of sides of the polygon, d the diameter of the polygon.

Experimental verification of this expression has recently been obtained in this laboratory using the profiles of carbon particles, and thus it can be concluded that a microscope of point-resolving power of 3 Å can resolve a 10 Å polygon of four sides provided that the transfer function allows constant contrast above 3 Å.

Radiation stability is a limiting factor for the resolution of many organic molecules. The only molecular images reported previously have been the highly radiation-resistant chlorinated copper phthalocyanine (Uyeda, Kobayashi, Suito, Harada & Watanabe, 1972) and our studies on non-chlorinated copper phthalocyanine (Murata, Fryer & Baird, 1976). This definition of molecular images excludes the biological molecules that are of comparable or greater sensitivity to radiation, but which are normally hydrogen-bonded structures and comprise many thousands of atoms. The relatively small molecules under consideration, *i.e.* aromatic hydrocarbons and phthalocyanines, have radiation stabilities in the range 0·1–30 C cm^{-2} (Claffey & Parsons, 1972; Reimer, 1960, 1961, 1965; Kobayashi & Reimer, 1975). The stability limits the resolution of the molecule in that the higher the resolution required the greater the number of information points (*i.e.* elastically scattered electrons) necessary. Thus if the number of electrons that will degrade the specimen is less than the number of information points for resolution of the molecule, then resolution is impossible. The ratio of these two quantities is unity at the 'critical exposure' level (Glaeser, 1975) though factors of noise and image-recording techniques will often require a factor of 5 for useful information to be obtained.

This is expressed as $Cd \geq 5/(fN_{cr})^{-1/2}$, where $C =$

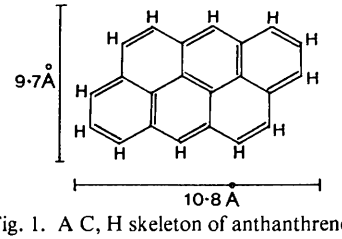

Fig. 1. A C, H skeleton of anthanthrene.

object contrast, d = minimum object size to be resolved, f = factor relating the number of electrons striking the object to the number providing useful information in the image, N_{Cr} = critical exposure (e Å^{-2}). Thus, substituting figures $C = 0{\cdot}1$, $f = 0{\cdot}25$, $N_{Cr} = 1{\cdot}25 \times 10^2$ e Å^{-2} (Glaeser, 1975) [this corresponds to 0·2 C cm^{-2}, a value for tetracene, a compound now known as naphthacene under IUPAC convention (Cahn, 1974)], $d = 8{\cdot}9$ Å.

This would correspond to the resolvable limit imposed by radiation damage and corresponds to the molecular diameter. Also, improvements in instrumental resolution, because an improvement in resolution means better definition between two points, means that constant C will be correspondingly improved. This is subject to transfer-function limitations, but improvements in instrumental resolution are of value. This assumes that radiation damage is a complete-molecular-disruption process. Initial steps such as crosslinking (Murata, Fryer, Baird & Murata, 1977), giving larger units, are usually so transitory as to be of little significance in resolution, though radiation-stabilized objects described by Johansen (1977) may be examples of this. Small improvements in the utilization factor might be possible but of little value. The contrast can be improved by spatial averaging over a large number of periodic unit cells (McLachlan, 1958; Kuo & Glaeser, 1975; Murata, Fryer & Baird, 1976). In the limit, of course, this is the process of X-ray and electron diffraction, but for structural information for small regions of the specimen, this method is of considerable value, and using a simple optical method with a photographic enlarger considerable improvements in contrast can be obtained.

The final limitation on resolution of small molecules lies in one's ability to prepare them in a suitable manner. A prerequisite for clear molecular definition is that in one orientation the molecules are superimposable, such that the electron beam is parallel to the axis of a column of molecules. For molecular crystals the space groups are not usually simple because of the requirement for maximum molecular contacts (Kitaigorodsky, 1961). Thus, planar molecules, for instance, will normally have the plane of the molecule at an acute angle to the column axis. As a result, expitaxic preparation of the crystals on a NaCl or KCl substrate (Ashida, 1966) will result in the plane of the molecule lying parallel to the substrate and the column axis at an angle to this plane. Viewing down the column, therefore, requires the specimen to be tilted with the corresponding disadvantages that this entails – particularly for minimal-exposure methods. Other specimen-preparation techniques have not proved suitable for molecular crystals. Crystallization from solution, for example, results in the molecular-column axes being parallel to the substrate, instead of normal to it as desired.

Anthanthrene was unusual in that expitaxic film formation occurred with the molecular columns normal to the substrate, such that minimal-exposure techniques could be employed (Williams & Fisher, 1970).

Consideration of the limitations of radiation damage shows that ideally the time during which the specimen is exposed to the electron beam is used only for image recording. Thus, focusing and astigmatism correction have to be carried out on an adjacent area of film, and for a tilted specimen the difference in height between the focused area and that to be recorded would have to be estimated. Therefore, minimal-exposure techniques on tilted specimens are very subject to error.

Experimental

The purified hydrocarbon anthanthrene (Clar, 1964) was sublimed under vacuum (1×10^{-5} Torr) on to cleaved KCl at room temperature. The organic film was backed with a thin layer of carbon, floated on to water, and collected on a 400 mesh copper grid. To obtain satisfactory specimens it was essential that both the organic layer and the carbon film were extremely thin. The anthanthrene was in the form of distinct crystals whose thickness was estimated to be less than 100 Å.

The electron microscopy was carried in a JEOL 100C microscope fitted with an ultra-high-resolution objective lens. This lens had a spherical aberration constant of 0·7 mm so that at 500 Å underfocus the phase-constant-transfer envelope was positive for periodicities of 3–20 Å. The details have been described elsewhere (Murata, Frayer & Baird, 1977). The electron-gun-shift controls had been modified by insertion of a switch and potentiometer so that the electron beam could be moved off and on the specimen without hysteresis or mechanical vibration. The image was recorded on Ilford G X-ray film. The minimal-exposure technique was as follows: (1) At very low magnification and low intensity a suitable grid square was located. This exposure was very brief and served to check that the support film was continuous with a high density of specimen present. (2) For one area of the film a large condenser aperture was inserted so that there was sufficient intensity to correct astigmatism at 850 000 × magnification. (3) A condenser aperture of 20 μm was inserted and at a magnification of 169 000× the specimen was focused. (4) The beam was switched to one side and the specimen moved to an unexposed region. A plate was brought forward and the shutter opened. After allowing the system to settle the beam was switched back and the plate exposed for approximately 1 s depending upon beam intensity. The intensity used was just sufficient to focus the specimen with well dark-adapted eyesight. No Faraday cage was fitted but the exposure lifetime of tetracene under these conditions was approximately 5 s for degradation of the

diffraction pattern, so the dose rate could be estimated at 4×10^{-2} C cm^{-2}.

Optical diffractograms were obtained using a He–Ne laser on a Polaron optical-diffractometer system.

Spatial averaging was carried out using a photographic enlarger. Enlarged negative transparencies of the original micrograph were used and prints made by briefly exposing the paper, moving the paper to another unit-cell position under safe-colour-mask illumination and exposing again. Random movement of the paper was made within the grid of the unit-cell projection such that after development up to 20 superimposed images were obtained. Care was taken to ensure that there was no preferred direction of movement of the paper that might give rise to an excessive error in this direction and an erroneous image.

Results and discussion

A high-resolution micrograph is shown in Fig. 2(*a*), together with the electron diffraction pattern (Fig. 2*b*) and the optical diffractogram (Fig. 2*c*). There is good agreement between the electron and optical diffraction patterns giving primary reflections of 12·1, 10·7 Å and β of 92°, which correspond to the (100) and (001) planes of the unit cell described by Smith & Stalley (1975). The optical diffraction pattern also is in good agreement with the calculated transfer function at an underfocus value of 500 Å. There are no contrast reversals down to 2·8 Å. Reflections of this order are shown in the diffractogram but the minimum spacing that can be discerned in the image is 4·8 Å. Also in the image, various changes in contrast occur that are probably caused by slight changes in diffraction conditions in different regions of the specimen. In the region marked *A* the orientation of the specimen is different from the other regions and occluded regions of varying orientation would give rise to strain, buckling and hence alteration of diffraction conditions throughout the crystal.

Fig. 3(*a*) shows an enlargement of the region *B* in Fig. 2. The micrograph is very noisy and averaging only 10 unit cells results in a considerable improvement (Fig. 3*b*). This should represent an improvement of $10^{1/2}$ in the signal-to-noise ratio, whilst Fig. 3(*c*), which represents the average of 20 unit cells, should be improved by a factor of 4·5. Qualitatively it does appear that this improvement is sustained but it is expected that continued improvement would be unlikely because of the cumulative errors introduced by the technique.

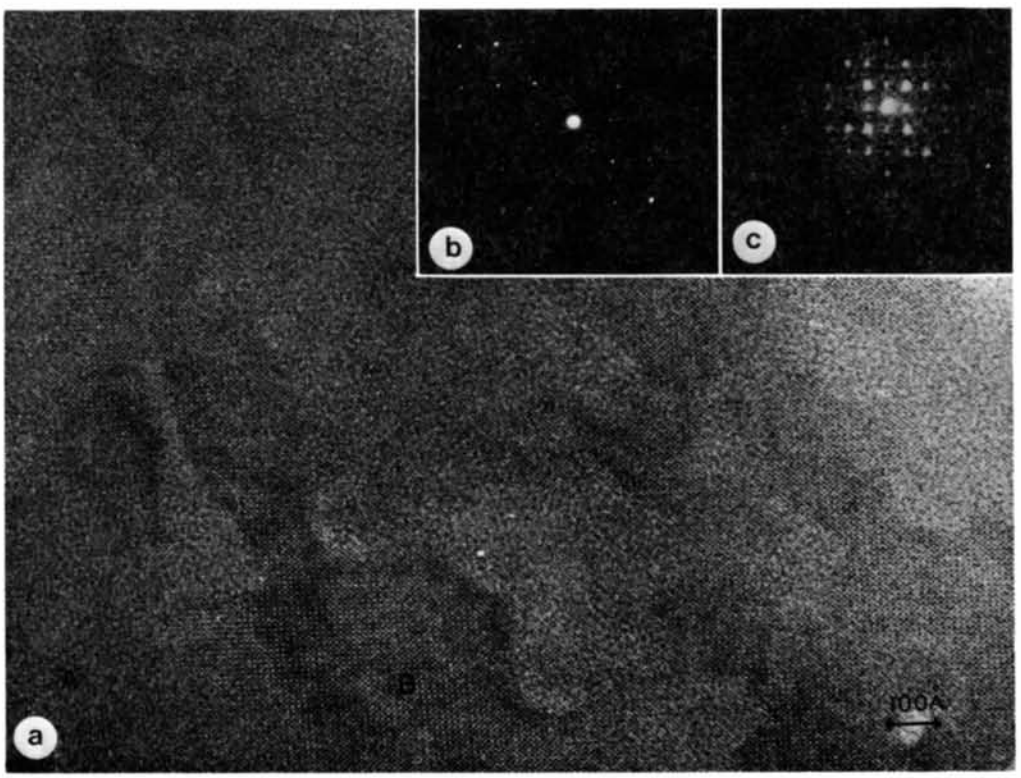

Fig. 2. (*a*) High-resolution micrograph of anthanthrene film, the majority of which is imaged parallel to the *b* axis. (*b*) Electron diffraction of anthanthrene film parallel to the *b* axis. (*c*) Optical diffraction of region *B* in (*a*).

Interpretation of the crystal structure in the light of the micrographs suggests that there are four columns of molecules at the corners of the unit cell – the micrograph representing a projection on the *ac* plane with the specimen being viewed parallel to the *b* axis. These molecules are rotated at an angle of approximately 30° to the *c* axis, as shown in Fig. 4. The centred molecule on the *ac* projection is nonequivalent and makes an angle of approximately 70° to the *c* axis, but this appears variable and possibly another molecule situated at $\frac{1}{2}, \frac{1}{2}, \frac{1}{2}$ is rotated relative to it. It must be stressed that the angles and molecular orientations in Fig. 4 are schematic although the micrograph is unambiguous about the molecular locations in the projection.

The radiation stability of this molecule in the microscope was comparable to tetracene, 0·2 C cm^{-2}, as judged by the fading of the electron diffraction spots. For both anthanthrene and tetracene the lifetime was approximately 5 s. The radiation-limited resolution is therefore approximately 9 Å, and the molecular dimensions of anthanthrene of 10·8 × 9·7 Å include the H atoms. The individual molecular resolution is quite distinct in the original micrograph such that the theoretical radiation-limited resolution of 9 Å would appear to be too conservative and that the assumed value for the object contrast *C* of 0·1 is too low. The shape is not well resolved, however, and shape information about this molecule and smaller molecules appears limited by instrumental performance. It would be expected that molecules of similar size and smaller than anthanthrene could be resolved in the microscope, but only as points, and that for molecules of this range of radiation stability the important feature is the instrumental resolution that is available. It should be noted that the radiation and shape limits to resolution refer to point resolution. Lattice resolution below these limits is possible as exemplified by the 4·8 Å resolution in Fig. 2(*a*).

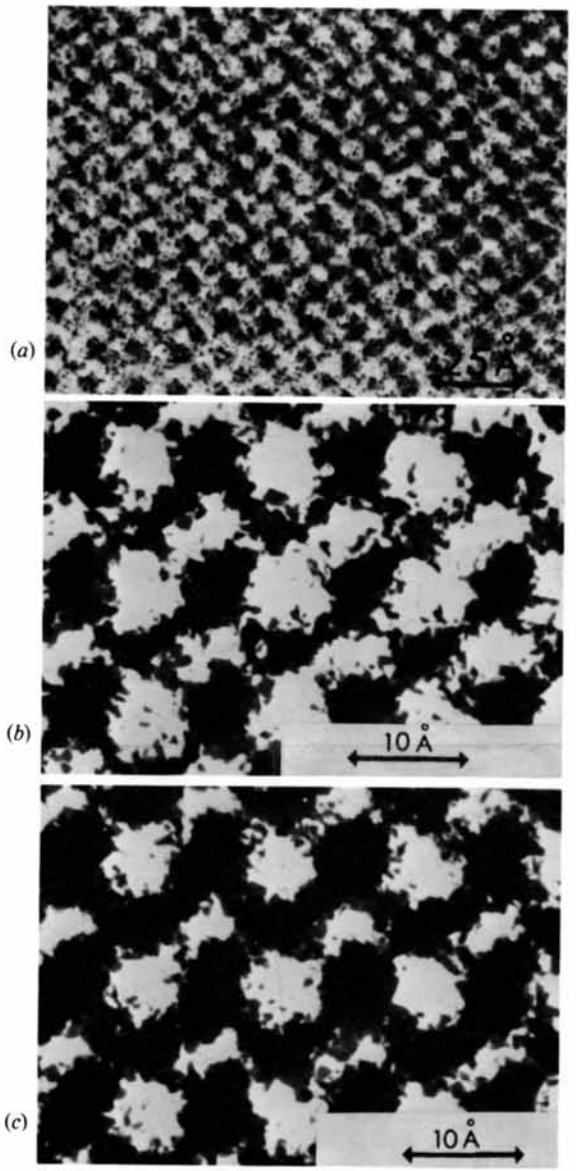

Fig. 3. (*a*) Enlarged micrograph of region *B* in Fig. 2(*a*). (*b*) Photographically averaged – 10 superimpositions. (*c*) Photographically averaged – 20 superimpositions.

I am grateful to the Science Research Council for a grant for equipment.

References

ASHIDA, M. (1966). *Bull. Chem. Soc. Jpn*, **39**, 2632–2638.

CAHN, R. S. (1974). *Introduction to Chemical Nomenclature*, 4th ed. London: Butterworths.

CLAFFEY, W. J. & PARSONS, D. F. (1972). *Philos. Mag.* **25**, 637–643.

CLAR, E. (1964). *Polycyclic Hydrocarbons*, Vol. 2, pp. 206–208. London: Academic Press.

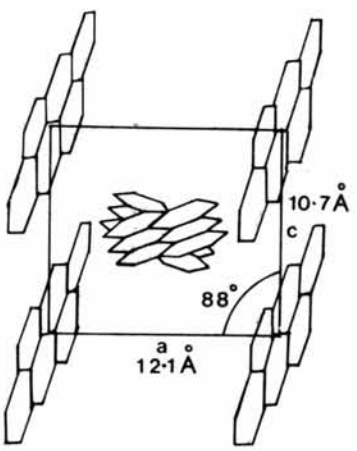

Fig. 4. Schematic representation of *ac*-plane projection.

COWLEY, J. M. (1972). *Physical Aspects of Electron Microscopy and Microbeam Analysis*, ch. 1, edited by B. SIEGEL & D. R. BEAMAN, pp. 3–15. New York: John Wiley.
GLAESER, R. M. (1975). *Physical Aspects of Electron Microscopy and Microbeam Analysis*, edited by B. SIEGEL & D. R. BEAMAN, ch. 12, pp. 205–229. New York: John Wiley.
JOHANSEN, B. V. (1977). *Ultramicroscopy*, **2**, 229–239.
KITAIGORODSKY, A. I. (1961). *Organic Chemical Crystallography*, pp. 94–105. New York: Consultants Bureau.
KOBAYASHI, T. & REIMER, L. (1975). *Bull. Inst. Chem. Res. Kyoto Univ.* **53**, 105–116.
KUO, I. A. M. & GLAESER, R. M. (1975). *Ultramicroscopy*, **1**, 53–66.
MCLACHLAN, D. (1958). *Proc. Natl. Acad. Sci. USA*, **44**, 948–956.
MURATA, Y., FRYER, J. R. & BAIRD, T. (1976). *J. Microsc.* **108**, 261–275.
MURATA, Y., FRYER, J. R., BAIRD, T. & MURATA, H. (1977). *Acta Cryst.* A**33**, 198–200.
MURATA, Y., FRYER, J. R. & BAIRD, T. (1977). *Proc. EMAG '77, Glasgow. Inst. Phys. Conf. Ser.* 36. ch. 3, pp. 127–130.
REIMER, L. (1960). *Z. Naturforsch. Teil A*, **15**, 405–411.
REIMER, L. (1961). *Z. Naturforsch. Teil B*, **16**, 166–170.
REIMER, L. (1965). *Lab. Invest.* **14**. 1082–1096.
ROSE, H. (1977). *Ultramicroscopy*, **2**, 251–267.
SMITH, G. W. & STALLEY, J. C. (1975). *Acta Cryst.* A**31**, S122.
UYEDA, N., KOBAYASHI, T., SUITO, E., HARADA, Y. & WATANABE, M. (1972). *J. Appl. Phys.* **43**, 5181–5189.
VON BORRIES, B. & KAUSCHE, G. A. (1940). *Kolloid Z.* **90**, 132–141.
WILLIAMS, R. C. & FISHER, H. W. (1970). *J. Mol. Biol.* **52**, 121–123.

Acta Cryst. (1978). A**34**, 607–609

Mixed-Layer Characteristics in Real Humite Structures

BY W. F. MÜLLER

Fachbereich 11, *Mineralogie, Technische Hochschule Darmstadt, Schnittspahnstrasse* 9, *D* 6100 *Darmstadt, Federal Republic of Germany*

AND H.-R. WENK

Department of Geology and Geophysics, University of California, Berkeley, California 94720, *USA*

(*Received* 20 *December* 1977; *accepted* 21 *February* 1978)

Transmission electron micrographs resolving (100) lattice fringes of clinohumite revealed faults parallel to (100). A simplified model of humite minerals, which interprets them as layers of forsterite and brucite–sellaite, was used for analysis of the faults. These compositional faults produce one or two unit layers of humite and/or chondrodite interlayered between the regular sequence of clinohumite along **a***. Thus, non-stoichiometric compositions of humite minerals can be explained as mixed layers.

Introduction

The structure of humite minerals with formula $n.Mg_2SiO_4.Mg(OH,F)_2$ consists basically of a slightly distorted hexagonal close packing of anions similar to olivine with an ordered O, F, and OH arrangement (Taylor & West, 1929). Octahedral interstices are partially filled with Mg(Ti,Fe), and tetrahedral ones with Si. The various structures can be classified by emphasizing either tetrahedral or octahedral building elements. Tetrahedral interstices are filled in alternate layers parallel to (100). Such a structure resembles the stacking of forsterite (Mg_2SiO_4) layers *F* with a spacing of 3·0 Å and brucite–sellaite [$Mg(F,OH)_2$] layers *B* with a spacing of 1·4 Å (Taylor & West, 1929). The stacking scheme applies only to the cations, anions are distributed over all layers equally. In norbergite the sequence is *FB* (d_{100} = 2 × 4·36 Å), in chondrodite *FFB* (d_{100} = 7·44 Å) (Fig. 1), in humite *FFFB* (d_{100} = 2 × 10·43 Å) and in clinohumite *FFFFB* (d_{100} = 13·44 Å). This model was shown to be oversimplified because order of octahedral positions which occupy half of the interstices is different in the various humite minerals (Ribbe, Gibbs & Jones, 1969). Octahedra filled with